Controlling the surface roughness of epitaxial SiC on silicon

N. Mishra,[1] L. Hold,[1] A. Iacopi,[1] B. Gupta,[2] N. Motta,[2] and F. Iacopi,[1,a]

[1]*Queensland Micro- and Nanotechnology Centre, Griffith University, Nathan, 4111 QLD, Australia*

[2]*Queensland University of Technology, 2 George Street, Brisbane 4001, QLD, Australia*

[a]*f.iacopi@griffith.edu.au*

ABSTRACT

The surface of cubic silicon carbide (3C-SiC) hetero-epitaxial films grown on the (111) surface of silicon is a promising template for the subsequent epitaxial growth of III-V semiconductor layers and graphene. We investigate growth and post-growth approaches for controlling the surface roughness of epitaxial SiC to produce an optimal template.

We first explore 3C-SiC growth on various degrees of offcut Si(111) substrates, although we observe that the SiC roughness tends to worsen as the degree of offcut increases. Hence we focus on post-growth approaches available on full wafers, comparing chemical mechanical polishing (CMP) and a novel plasma smoothening process. The CMP leads to a dramatic improvement, bringing the SiC surface roughness down to sub-nanometer level, though removing about 200nm of the SiC layer. On the other hand, our proposed HCl plasma process appears very effective in smoothening selectively the sharpest surface topography, leading up to 30% improvement in SiC roughness with only about 50 nm thickness loss. We propose a simple physical model explaining the action of the plasma smoothening.

I. INTRODUCTION

Over the last decade, the cubic silicon carbide (3C-SiC) heteroepitaxial films on (111) silicon surfaces have attracted considerable interest as a pseudo-substrate for the subsequent growth of epitaxial III-V semiconductors (e.g. AlN, GaN etc.) and graphene layers[1-4].

The III-nitrides find promising applications in the area of power electronics, micro-electrical-mechanical and opto-electronic systems[5-7]. Graphene has countless exciting applications from sensing to photonics[8-10]. However, large scale industrial applications of III-nitrides and graphene are limited by the necessity of expensive substrates (such as sapphire, bulk SiC, or GaN) to obtain good quality epitaxial growth[2,11].

High quality silicon substrates are available in sizes up to 12 inches and are relatively inexpensive. Further, atoms on the Si(111) surface are arranged in an hexagonal configuration, analogous to that of III-nitrides (AlN, GaN etc.)[12]. However, epitaxial III-nitrides layers such as GaN grown on Si(111) suffer from poor quality due to the stress induced by the large lattice mismatch (~17%) and difference in thermal expansion coefficient (~33%) between GaN and Si. On the other hand, by employing epitaxial 3C-SiC on Si as a template, a better quality epitaxial GaN is expected, due to the comparatively smaller (3%) lattice mismatch between GaN and 3C-SiC(111)[1]. This is valid also for epitaxial graphene, whose structural coherency with 3C-SiC(111) makes it a promising material for next-generation nano-electronic devices [13,14].

Nevertheless, epitaxial growth onto 3C-SiC/Si is still affected by factors such as crystalline defects in the 3C-SiC films and surface roughness. It is well known that 3C-SiC heteroepitaxy on Si is typically characterized by a large number of crystallographic defects such as stacking faults, dislocations, and twins[15-17]. The nucleation of such defects is largely due to the lattice mismatch difference between 3C-SiC and Si which is about 20%[5]. Stacking faults and twinning appearing at the film surface are common contributors to undesired

roughening of the SiC epitaxial films. Defects and roughness at the free surface of SiC will strongly affect the subsequent epitaxial of graphene[18]. Increasing surface roughness is reported to adversely affect the defect density and electron mobility in the GaN and graphene layers on SiC/Si[19-22].

The improvement of the smoothness of epitaxial SiC on Si films can be pursued at two stages: 1) upon film growth (e.g. by optimizing the growth process and growth surfaces[21,23,24]); 2) through post-growth processes[25,26]. Among the available post-growth processes, chemical mechanical polishing (CMP) using diamond based slurries is very effective at reducing roughness to a level suitable for device fabrication[25]. However, it is difficult to avoid surface scratches, due to the high hardness of the diamond particles. To overcome this problem, Deng and Yamamura have proposed a plasma assisted polishing technique[26]. In this process, oxidation by atmospheric water vapour plasma and polishing by soft abrasive is used to obtain an atomically smooth surface without scratches and subsurface damages. Still, this process suffers from the high cost of the SiC polishing process and the considerable loss of SiC thickness usually required to obtain an optimal smoothness.

In this work, we first investigate the growth of epitaxial SiC onto Si(111) with different degrees of offcut and subsequently we compare the action of a commercial SiC CMP process (NOVASiC, France) with a novel inductively coupled plasma smoothening process to improve the surface roughness of 3C-SiC. We show that although the CMP process yields the best achievable smoothening, our proposed plasma process still offers a considerable improvement of surface roughness through a cheaper, faster and cleaner process.

II. EXPERIMENTAL

Unintentionally doped thick 3C–SiC films were grown on <111> oriented on-axis and offcut Si wafers (2 inch) in a hot-wall horizontal low pressure chemical vapour deposition

reactor though an alternate supply epitaxy with SiH_4 and C_3H_6 at 1000°C. The SiC growth process is fully described by Wang *et al.*[15]. The details regarding the orientation and degree of offcut of the used Si substrates are shown in Table I.

Subsequently, we exposed the 250nm thick SiC films grown on different substrates as per Table I to a 30s plasma process at room temperature in an inductively coupled plasma (ICP) system by STS. The samples were introduced in the chamber on a 6 inch wafer carrier. We used 50 sccm HCl gas flow to maintain a chamber pressure of 4 mTorr, while the radio frequency (RF, 13.56 MHz) source power was set at 100 W. We have already successfully used an analogous HCl ICP process for etching the 3C-SiC in a very controlled and uniform fashion at the wafer- scale[27]. The exposure of SiC films to the HCl plasma for 30 seconds results in the removal of about 50 nm of the as-grown film thickness. Note that the ICP process generates a highly anisotropic plasma, thanks to the substrate bias and the low operating chamber pressure.

In parallel, a thicker (~1 μm) 3C-SiC epitaxial film was grown on on-axis Si(111) substrate (sample 6 in Table I), to receive a commercially available chemical-mechanical-polishing process, followed by a surface cleaning, at NOVASiC (Le Bourget du Lac, France[28]). The film intended for CMP was prepared considerably thicker to accommodate for the extensive thickness loss expected from the polishing.

Atomic force microscopy (AFM) measurements were performed to analyse the surface of the 3C-SiC films using an NT-MDT NTEGRA and a Park NX20 systems, operated in non-contact and contact mode, respectively. While both AFM equipment yield equivalent information in terms of surface roughness, the Park system was used on selected samples to perform a power spectral density analysis with superior accuracy.

We chose to report throughout this paper the root-mean-square (RMS) values and average peak-to-valley heights measured on 5x5 μm^2 scan sizes with 256 x 256 resolution

with the NT-MDT NTEGRA system. Measurements were performed in non-contact mode with a single crystal silicon probe with tip curvature radius of 10 nm.

The Park NX20 system was used in contact mode to extract high resolution power spectral densities (PSD). A PSD curve gives the relative strength of each roughness component of a surface microstructure as a function of its spatial frequency. The Park microscope is equipped with a single crystal silicon cantilever length 125 μm and tip radius of curvature <10 nm, operated at a frequency of 360 kHz and scan rate of 0.3 Hz. The power spectral densities were analysed using the XEI 1.8.0.Build32 software from 5x5 μm^2 scan sizes with 512 x 512 resolution.

III.RESULTS AND DISCUSSION

A. Analysis of 3C-SiC films grown on on-axis and offcut Si(111)

In order to examine the influence of the degree of offcut substrates on the surface of 3C-SiC films, we compare the surface morphology and RMS roughness.

Figure 1 shows the trend of the RMS surface roughness for the 250nm epitaxial SiC films versus the degree of offcut of the Si(111) substrates on which they were grown. The solid line in the graph indicates that the SiC surface roughness tends to increase with an increasing degree of offcut. The measured RMS roughness of the SiC film grown on the on-axis substrate is around 2.6 nm, reaching up to 3.3 nm for the film grown on a 10° offcut wafer.

The surface morphologies as measured with the NT-MDT system are compared in Fig. 2. Fig. 2(a) shows the surface of the 3C-SiC film grown on the on-axis Si (111) substrate (sample 1 in Table I). The triangular patterns uniformly distributed on the surface, more evident on the 0.25x1 μm^2 scan, are related to the propagation of twins and stacking faults to

the surface and confirm the three fold symmetry of underlying Si (111) substrate[29]. A height profile extracted from the 5x5 μm^2 scan is also shown. The average peak-to-valley height evaluated from this film is around 29 nm.

As the degree of offcut of the Si substrate increases, we observe the gradual appearance of more elongated patterns on the epitaxial SiC surface, as shown for the film grown on the Si(111) with a 5° offcut in Fig.2(b), 5x5 μm^2 scan. The corresponding 0.25x1 μm^2 scan in Fig.2(b) still does show triangular patterns, though blurred. For the SiC film grown on a Si(111) surface with 10° offcut (sample 3, Table I), strain-driven bunching of the pre-existing substrate steps results in a rippled morphology as shown in Fig. 2(c). The ripples are characterized by a mean peak-to-peak distance and average peak-to-valley height of about 200 nm and 45 nm respectively. According to previous reports, the observed ripples could be either running parallel[30] or orthogonal[31] to the substrate steps. The higher resolution scan in Fig. 2(c) also shows that the surface morphology no longer shows triangular patterns, but only irregular –shaped asperities. This sample shows the highest surface roughness (sample 5, Table I).

Our observation of an overall worsening of the RMS roughness versus an increasing degree of substrate offcut seems to contradict previous reports[23]. This discrepancy is attributed to substantially different epitaxial growth conditions, such as a considerably lower growth temperature in our case (1000°C).

B. Plasma smoothening

We analyze the surface morphology and roughness of the SiC films after exposure to a 30s HCl plasma process. The RMS roughness values after plasma exposure are shown by the dashed line in Fig.1 and also reported in Table I (samples 1 to 5).

Figure 1 indicates that the surface roughness after plasma smoothening improved up to 23% and 30% for SiC films grown on on-axis and 10° offcut substrates, respectively. Accordingly, the average peak-to-valley excursion is also found reduced after the plasma process (Table I), in particular it is almost halved for the SiC film on the 10° offcut silicon wafer. A somewhat less significant improvement is observed for the films grown on substrates with intermediate offcut. An explanation for this will be offered with the help of the power spectral analysis in the next section.

Figure 3 compares the 3D AFM images of the 3C-SiC film onto an on-axis Si(111) (sample 1 in Table I) as-grown (a) and after the HCl plasma smoothening (b). The image in Fig. 3(b) shows the predominance of broader asperities as compared to Fig. 3(a). Figure 4 also shows the size distribution histogram of surface asperities belonging to sample 1 after plasma smoothening (dotted line) shifting towards larger size with respect to the as-grown sample, confirming the visual feature broadening indicated by the 3D image in Fig.3.

We propose a simple mechanism to explain the smoothening action provided by the short HCl plasma etching in Fig.5. The substrate in the ICP system is subject to an RF bias, which accelerates the ionized species in the gas generating a strongly directional plasma. The substrate voltage will induce charges at the sample surface. The presence of sharp asperities at the surface of the as-grown SiC films, i.e. portions with a highly curved surface, will induce locally higher charge densities. Therefore, the highly energetic H^+ and Cl^- ions from the plasma will be accelerated preferentially towards those sharp asperities as opposed to the "valley" portions of the SiC surface, locally increasing the ion-assisted etching action of the HCl plasma and forming volatile compounds ($SiCl_4$, SiH_4, CH_4 etc.). Therefore, we suggest that the 3C-SiC surface is smoothened by the HCl plasma by removing the sharpest asperities at a much higher rate than the remaining SiC surface.

C. Chemical mechanical polishing and power spectral analysis

CMP is a very effective technique to reduce the surface roughness for most thin films. We compare the surface of the thick epitaxial SiC grown on an on-axis Si(111) wafer with AFM (sample 6 in Table I) before and after being polished at NOVASiC (France).

As expected from the symmetry of the Si(111) substrate, the surface of the as-grown thick SiC film on on-axis also showed marked triangular patterns as the 250nm film on the same substrate type (AFM image is not shown here). However, the RMS roughness of the as-grown 1 μm thick film showed a considerably higher value (around 5 nm) as compared to 2.6 nm of the thinner film (samples 1 and 6 in Table I). This is not uncommon in the epitaxial growth of SiC films[32]. After the CMP process, the SiC RMS roughness reduced dramatically from 5 nm to a sub-nanometer level (0.7 nm), leading to a colossal 86% reduction of surface roughness and average peak-to-valley reduction from 45 nm down to 7 nm. Note that the polishing removed approximately the top 200 nm of the SiC layer.

RMS roughness and average peak-to-valley data from the analysis of an AFM measurement carry mostly information about excursions in the z-axis of the scan, however they do not define the in-plane surface morphology, which is another key parameter to be taken into account for subsequent epitaxial growth. Hence, for a detailed understanding of the smoothening action of the CMP process versus that of the HCl plasma process, we compare the power spectral densities of the surfaces of samples 1, 3 and 6, as-grown and after plasma or CMP. This comparison is shown in Fig. 6.

The PSD curves for the on-axis films (sample 1) as-grown and after plasma smoothening appear mostly overlapping over the lower frequency range (Fig. 6 (a)), i.e. for frequencies below roughly 7 μm^{-1}. However, the PSD curve of the sample after plasma process drops significantly over the high frequency range. This reduction confirms the selective etching by the plasma of the sharpest features present on the as-grown SiC surface

hypothesised in the previous section. Further, we can observe that the spectrum corresponding to the as-grown film on the 5° offcut Si(111) (sample 3, Table I) shows a substantially less prominent contribution of high frequencies (above 7 μm^{-1}) the total surface roughness of the film as compared to the as-grown sample 1. After plasma smoothening, both curves for sample 1 and 3 coincide, indicating that the plasma action is equivalent in both cases. However, the plasma still results in a less pronounced net smoothening for sample 3 (Table I), as its starting roughness is not as influenced by sharp asperities as sample 1.

Therefore, we can confidently conclude that most the smoothening originated from the plasma process is a result of the preferential etching of surface asperities with spatial frequencies above 7 μm^{-1}, leading to an effective improvement of short –ranged roughness with wavelength equal or smaller than 150 nm. Note that the improvement of the short –ranged roughness component of SiC films may prove to be more critical than the larger range topography in terms of obtaining a suitable surface for subsequent high quality epitaxial growth.

Finally, the PSD after CMP in Fig. 6(b) shows substantially lower values across all of the investigated spatial frequencies as compared to the as-grown thick SiC film, indicating that the colossal roughness reduction in the CMP case is a result of a homogeneous smoothening across broad and sharp surface asperities. Preliminary comparisons of graphene grown from a pristine on-axis SiC(111) surface (sample 1) and from a polished SiC(111) surface (sample 6) following the procedure we reported in Gupta et al.[3], indicate that the original surface roughness is conserved in both cases after Si sublimation at 1250˚C, yielding 2.4 nm and 0.8 nm RMS roughness, respectively. This is very encouraging as it proves that an atomic -scale smooth graphene can be obtained from epitaxial SiC on Si by optimizing the initial SiC film roughness.

IV. CONCLUSIONS

We explored growth and post-growth approaches for improving the surface roughness and morphology of heteroepitaxial 3C-SiC films on Si(111) for their use as templates for III-nitrides and graphene growth on silicon substrates.

No improvement in surface roughness, but rather a worsening, is observed when 3C-SiC is grown on offcut Si(111) substrates. Hence, we propose a novel method through a HCl plasma smoothening and we compare its efficacy to that of a chemical-mechanical-polishing process commercially available through NOVASiC, France. The commercial CMP process confirms the ability to produce a SiC surface with sub-nanometer roughness by removing effectively asperities across a wide range of spatial frequencies. Nevertheless, our proposed plasma smoothening demonstrates high efficacy in selectively removing the sharpest asperities from the 3C-SiC surface. We obtained up to 30% reduction in RMS roughness by this method, and explained that the extent of efficacy depends on the weight of the contribution of short –ranged roughness of the initial film. A simple physical mechanism is suggested to explain surface smoothening with the HCl –based plasma process.

We conclude that as the proposed plasma smoothening is faster, cleaner and does not require the highly specialized equipment and know-how related to CMP processes, it still represents an appealing smoothening approach whenever the quality of subsequent epitaxial processes are mostly threatened by short –ranged roughness. Additionally, the total SiC film thickness loss by plasma smoothening is significantly reduced to about 50nm, as compared to roughly 200nm loss for the CMP process.

The detailed understanding and control of surface roughness of heteroepitaxial SiC on Si by wafer–scale plasma and CMP processes will provide crucial pathways to grow quality III-V semiconductor or graphene epitaxial layers on silicon wafers for technological

applications. For example, we disclose the achievement of an atomically flat graphene through sublimation from 3C-SiC films with optimized surface roughness, enabling graphene on silicon wafers with potentially highly improved electronic properties as suggested by the work of Kang et al.[33]

ACKNOWLEDGEMENTS

Sincere thanks to Atieh Ranjbar Kermany, Glenn Walker and Dr. Ben Cunning for their valuable support. The authors acknowledge the support from the Australian National Fabrication Facility (ANFF) and SPTS Technologies (San Jose, Ca). Dr. F. Iacopi is the recipient of an Australian Research Council Future Fellowship (FT120100445). The authors acknowledge also ARC for funding through the DP130102120 and the Queensland Government through the Smart Futures Fellowships Program.

REFERENCES

[1]J. Komiyama, Y. Abe, S. Suzuki, and H. Nakanishi, Applied Physics Letters **88**, 091901 (2006).

[2]W. A. De Heer, C. Berger, M. Ruan, M. Sprinkle, Y. Hu X. Li, B. Zhang, J. Hankinson, and E. Conrad, PNAS **108,** 16900 (2011).

[3]B. Gupta, M. Notarianni, N. Mishra, M. Shafiei, F. Iacopi, and N Motta, Carbon **68**, 563 (2014).

[4]V. Y. Aristov, G. Urbanik, K. Kummer, D. V. Vyalikh, O. V. Molodtsova, A. B. Preobrajenski, A. A. Zakharov, C. Hess, T. Hänke, B. Büchner, I. Vobornik, J. Fujii, G. Panaccione, Y. A. Ossipyan, and M. Knupfer, Nano letters **10,** 992 (2010).

[5]V. Cimalla, J. Pezoldt, and O. Ambacher, Journal of Physics D: Applied physics **40**, 6386 (2007).

[6]S. Nakamura, M. Senoh, S. Nagahama, N. Iwasa, T. Yamada, T. Matsushita, Y. Sugimoto, and H. Kiyoku, Applied physics letters **70**, 1417 (1997).

[7]W. Saito, Y. Takada, M. Kuraguchi, K. Tsuda, I. Omura, T. Ogura, and H. Ohashi, Electron Devices, IEEE Transactions on **50**, 2528 (2003).

[8]F. Schwierz, Nature Nanotechnology **5**, 487 (2010).

[9]A. B. Kuzmenko, E. van Heumen, F. Carbone, and D. van der Marel, Physical Review Letters **100**, 117401 (2008).

[10]J. D. Fowler, M. J. Allen, V. C. Tung, Y. Yang, R. B. Kaner, and B. H. Weiller, Acs Nano **3**, 301 (2009).

[11]M. C. Luo, J. M. Li, Q. M. Wang, G. Sh. Sun, L. Wang, G. R. Li, Y. P. Zeng, and L. Y. Lin, Journal of Crystal Growth **249**, 1 (2003).

[12]S. A. Nikishin, V. G. Antipov, S. Francoeur, N. N. Faleev, G. A. Seryogin, V. A. Elyukhin, H. Temkin, T. I. Prokofyeva, M. Holtz, and A. Konkar, Applied physics letters **75**, 484 (1999).

[13]A. Ouerghi, R. Belkhou, M. Marangolo, M. G. Silly, S. E. Moussaoui, M. Eddrief, L. Largeau, M. Portail, and F. Sirotti, Applied physics letters **97**, 161905 (2010).

[14]H. Fukidome, S. Abe, R. Takahashi, K. Imaizumi, S. Inomata, H. Handa, E. Saito, Y. Enta, A. Yoshigoe, Y. Tareoka, M. Kotsugi, T. Ohkouchi, T. Kinoshita, S. Ito, and M. Suemitsu, Applied Physics Express **4**, 115104 (2011).

[15]L. Wang, S. Dimitrijev, P. Tanner , J. Han, A. Iacopi, L. Hold, and B. H. Harrison, Thin Solid Films **519**, 6443 (2011).

[16]K. C. Kim, C. Il Park, J. Il Roh, K. S. Nahm, and Y. H. Seo, Journal of Vacuum Science & Technology A: Vacuum, Surfaces, and Films **19**, 2636 (2001).

[17]F. Iacopi, G. Walker, L. Wang, L. Malesys, S. Ma, B. V. Cunning, and A. Iacopi, Applied physics letters **102**, 011908 (2013).

[18]A. Ouerghi, A. Balan, C. Castelli, M. Picher, R. Belkhou, M. Eddrief, M. G. Silly, M. Marangolo, A. Shukla, and F. Sirotti, Applied physics letters **101**, 021603 (2012).

[19]Y. M. Lin, C. Dimitrakopoulos, K. A. Jenkins, D. B. Farmer, H. Y. Chiu, A. Grill, and P. Avouris, Science **327**, 662 (2010).

[20]J. X. Wang, S. Y. Yang, J. Wang, J. P. Lui, Z. W. Li, H. J. Li, D. D. Jin, X. L. Liu, Q. S. Zhu, and Z.G. Wang, Chinese Physics B **22**, 077305 (2013).

[21]M. Fanton, J. Robinson, B. Weiland, and J. Moon, ECS Transactions **19**, 131 (2009).

[22]H. Fukidome, Y. Kawai, H. Handa, H. Hibino, H. Miyashita, M. Kotsugi, T. Ohkochi, M. Jung, T. Suemitsu, T. Kinoshita, T. Otsuji, and M. Suemitsu, Proceedings of the IEEE **101**, 1557 (2013).

[23]A. Severino, M. Camarda, G. Condorelli, L. M. S. Perdicaro, R. Anzalone, M. Mauceri, A. L. Magna, and F. L. Via, Applied physics letters **94**, 101907 (2009).

[24]J. A. Powell, L. G. Matus, M. A. Kuczmarski, C. M. Chorey, T. T. Cheng, and P. Pirouz, Applied physics letters **51**, 823 (1987).

[25]A. A. Yasseen, C. A. Zorman, and M. Mehregany, Journal of The Electrochemical Society **146**, 327 (1999).

[26]H. Deng and K. Yamamura, Current Applied Physics **12,** Supplement 3, S24 (2012).

[27]F. Iacopi, R. E. Brock, A. Iacopi, L. Hold, and R. H. Dauskardt, Acta Materialia **61**, 6533 (2013).

[28]http://www.novasic.com/services/polishing/polishing.php.

[29]R. Anzalone, C. Bongiorno, A. Severino, G. D'. Arrigo, G. Abbondanza, G. Foti, and F. L. Via, Applied physics letters **92**, 224102 (2008).

[30]C. Teichert, Physics Reports **365**, 335 (2002).

[31]A. Pimpinelli, A. Videcoq, and M. Vladimirova, Applied surface science **175–176**, 55 (2001).

[32]H. Omi, Y. Homma, V. Tonchev, and A. Pimpinelli, Physical Review Letters **95**, 216101 (2005).

[33]H.-C. Kang, H. Karasawa, Y. Miyamoto, H. Handa, H. Fukidome, T. Suemitsu, M. Suemitsu, T.Otsuji, Solid State Electronics **54**, 1071 (2010).

LIST OF TABLES

Table I. Epitaxial 3C-SiC films grown on various Si(111) substrate types used in this study. Degree, and direction of offcut of the silicon substrates, and SiC film thickness are indicated, together with the RMS roughness values and average peak-to-valley excursions for the as-grown films and those after plasma (or CMP for sample 6) smoothening.

Sample No.	Offcut (±0.5°)	Offcut Direction	3C-SiC as-grown thickness (nm)	RMS roughness (±0.15 nm)		Average peak-to-valley (±2.1 nm)	
				As-grown	After smoothening	As-grown	After smoothening
1	0	----	250	2.6	2.0	28.8	22
2	1.5	[-1 -1 2]	250	2.4	2.3	25.8	28.6
3	5	[-1 -1 2]	250	2.7	2.4	26.8	26.5
4	9.45	[-1 -1 2]	250	2.9	2.7	26.2	26.2
5	10	[1 1 2]	250	3.3	2.3	45.6	21.4
6*	0	----	1000	5.1	0.7	44.8	6.6

FIGURE CAPTIONS

FIG. 1. RMS roughness of 250 nm thick 3C-SiC grown on on-axis and off-axis Si(111) substrates. Solid and dashed lines indicate the RMS values of films as-grown and after plasma smoothening, respectively.

FIG. 2. Surface morphology of 3C-SiC epitaxial films grown on (a) on axis, (b) 5° offcut towards [-1 -1 2], and (c) 10° offcut towards [1 1 2] Si(111) substrates. The images on the left and the top right edges are 5x5 μm^2 and 0.25x1 μm^2 AFM scans, respectively. Height profiles extracted from 5x5μm^2 scans are shown in the bottom right graph.

FIG. 3. 3D AFM micrographs of 3C-SiC films on on-axis Si(111): (a) as-grown, (b) after plasma smoothening. The sharpest asperities present in (a) are not found in (b), after plasma smoothening.

FIG. 4. Histograms showing the in-plane size distribution of surface asperities of 3C-SiC on on-axis Si(111): as-grown (solid curve) and after plasma smoothening (dashed curve). After smoothening the histogram shifts towards larger dimensions indicating larger average asperities.

FIG. 5. Proposed SiC plasma smoothening mechanism. The RF power supply connected to the substrate during the plasma process will induce higher charge densities at the sharply curved surface portions (shown by circle). The ions generated in the plasma from the HCl gas will preferentially etch the sharpest asperities of the SiC film resulting in a selective surface smoothening.

FIG. 6. Power spectral densities of 3C-SiC films on on-axis Si(111): (a) 250nm thick (sample 1 and 3), as-grown and after plasma smoothening and, (b) 1 μm thick, as-grown and after CMP. Whereas the CMP smoothens surface asperities over the full range of investigated frequencies, the plasma process smoothens selectively only the finest surface topography (spatial frequencies beyond 7 μm^{-1}).

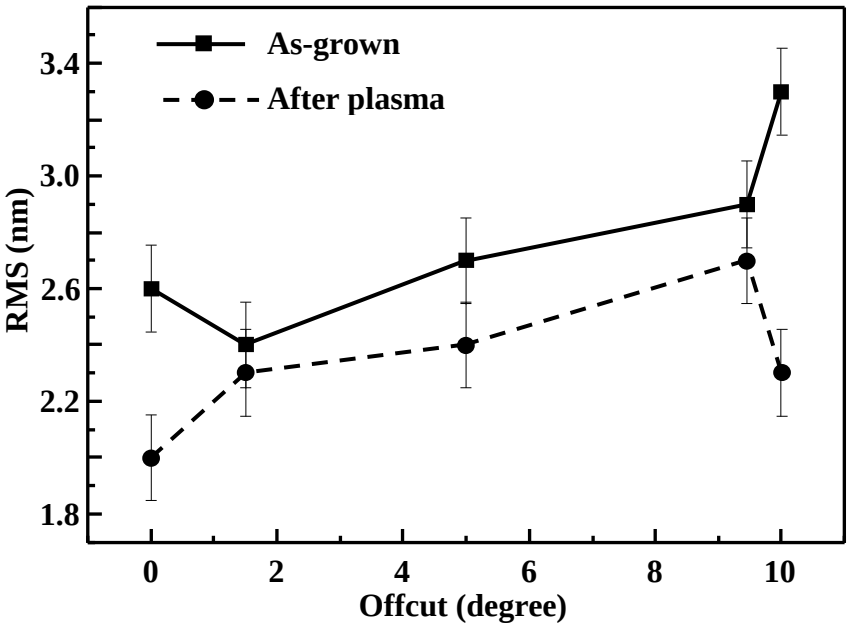

FIG. 1. RMS roughness of 250 nm thick 3C-SiC grown on on-axis and off-axis Si(111) substrates. Solid and dashed lines indicate the RMS values of films as-grown and after plasma smoothening, respectively.

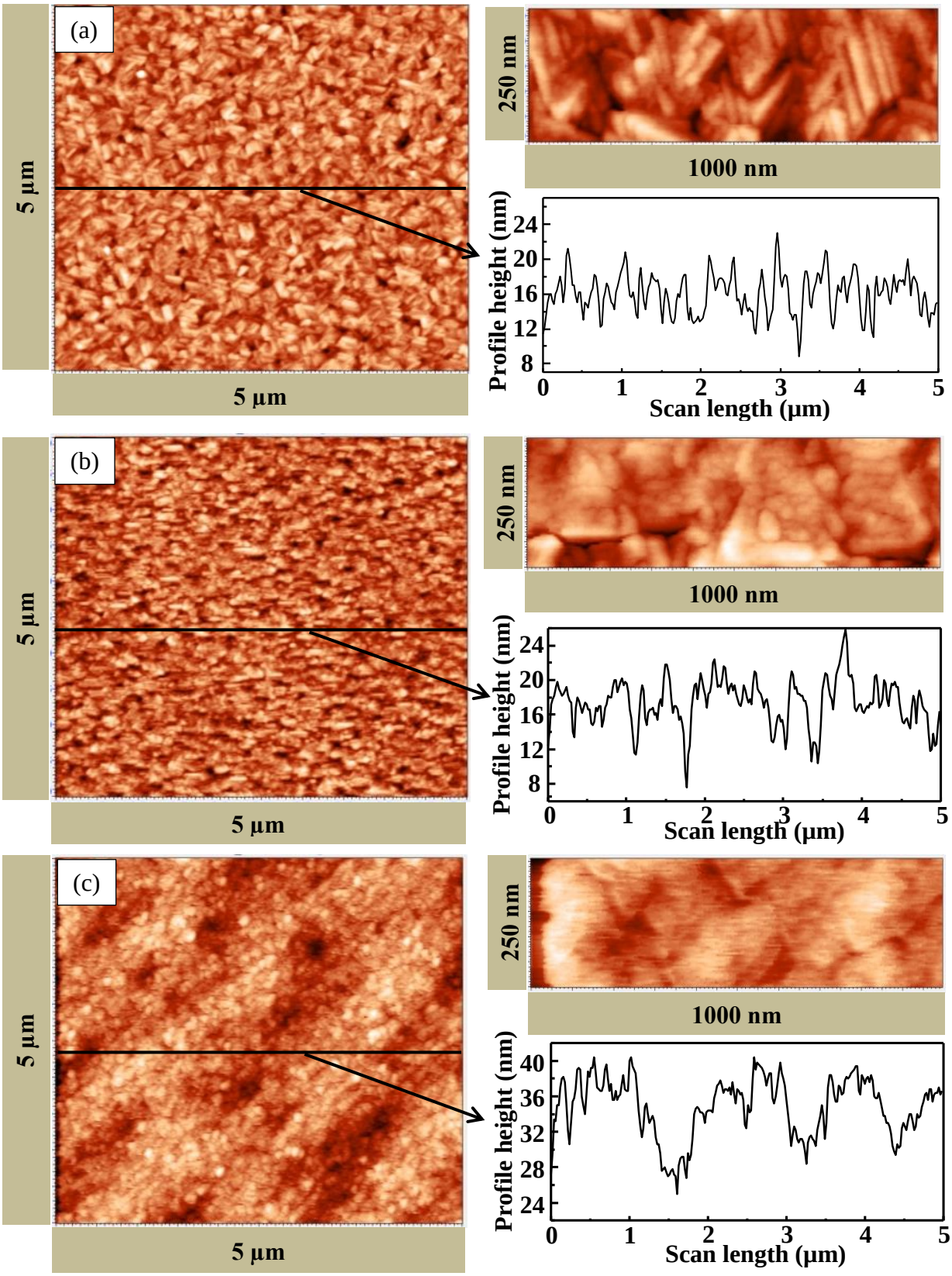

FIG. 2. Surface morphology of 3C-SiC epitaxial films grown on (a) on axis, (b) 5° offcut towards [-1 -1 2], and (c) 10° offcut towards [1 1 2] Si(111) substrates. The images on the left and the top right edges are 5x5µm^2 and 0.25x1µm^2 AFM scans, respectively. Height profiles extracted from 5x5µm^2 scans are shown in the bottom right graph.

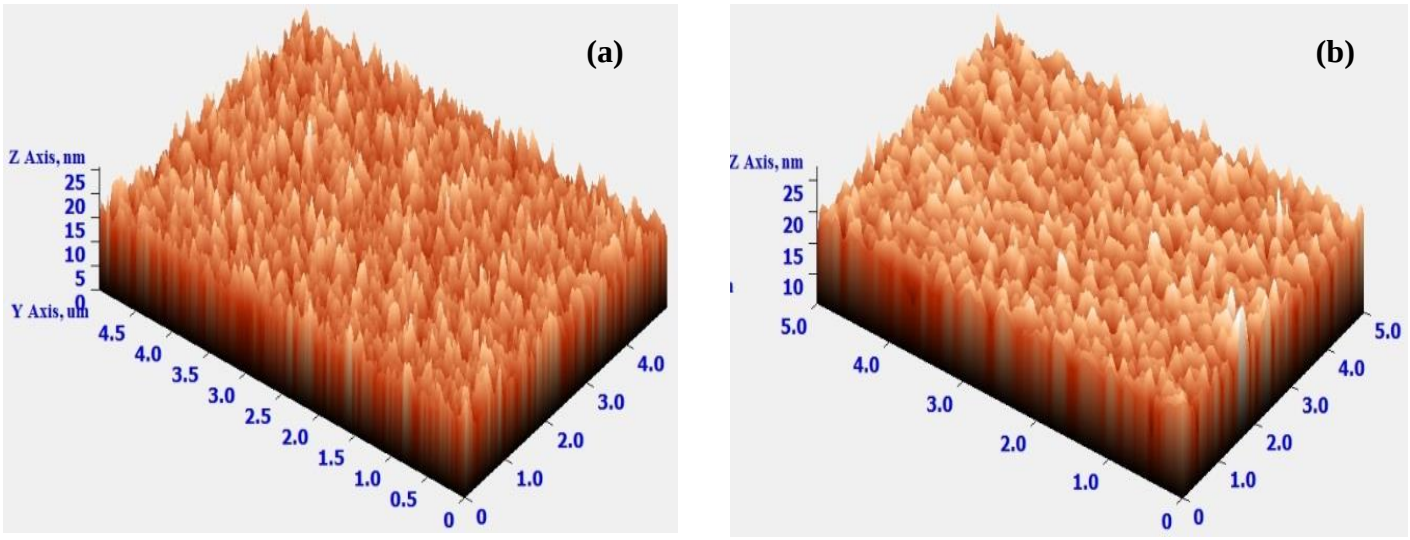

FIG. 3. 3D AFM micrographs of 3C-SiC films on on-axis Si(111): (a) as-grown, (b) after plasma smoothening. The sharpest asperities present in (a) are not found in (b), after plasma smoothening.

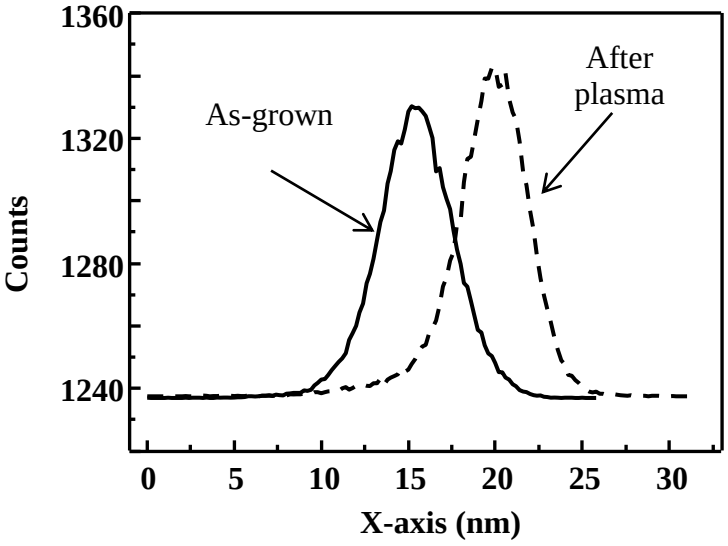

FIG. 4. Histograms showing the in-plane size distribution of surface asperities of 3C-SiC on on-axis Si(111): as-grown (solid curve) and after plasma smoothening (dashed curve). After smoothening the histogram shifts towards larger dimensions indicating larger average asperities.

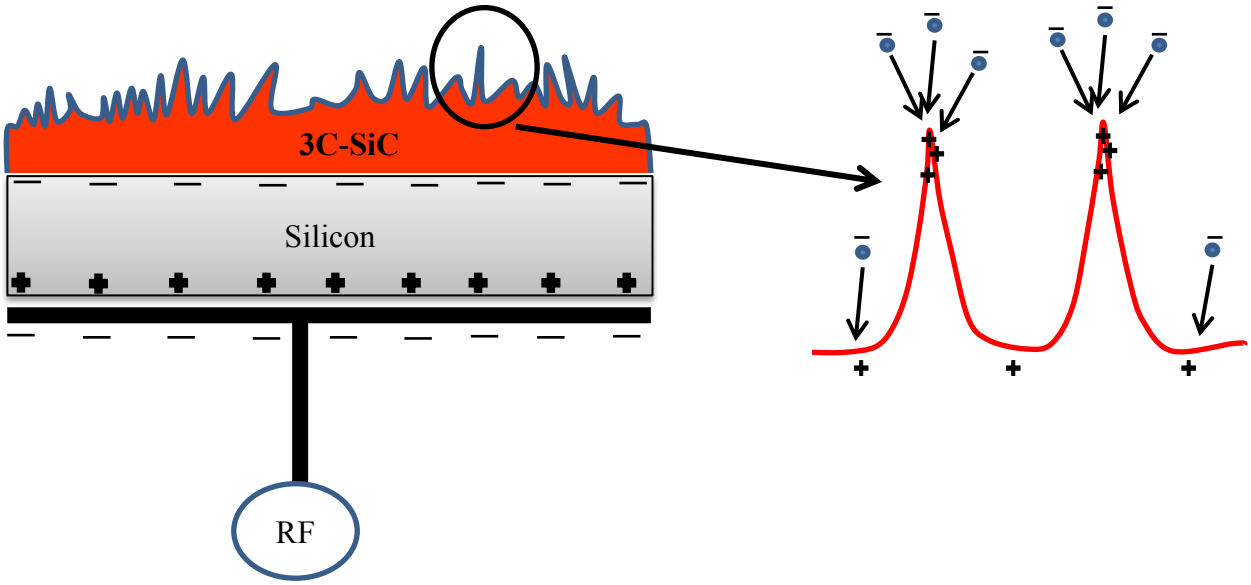

FIG. 5. Proposed SiC plasma smoothening mechanism. The RF power supply connected to the substrate during the plasma process will induce higher charge densities at the sharply curved surface portions (shown by circle). The ions generated in the plasma from the HCl gas will preferentially etch the sharpest asperities of the SiC film resulting in a selective surface smoothening.

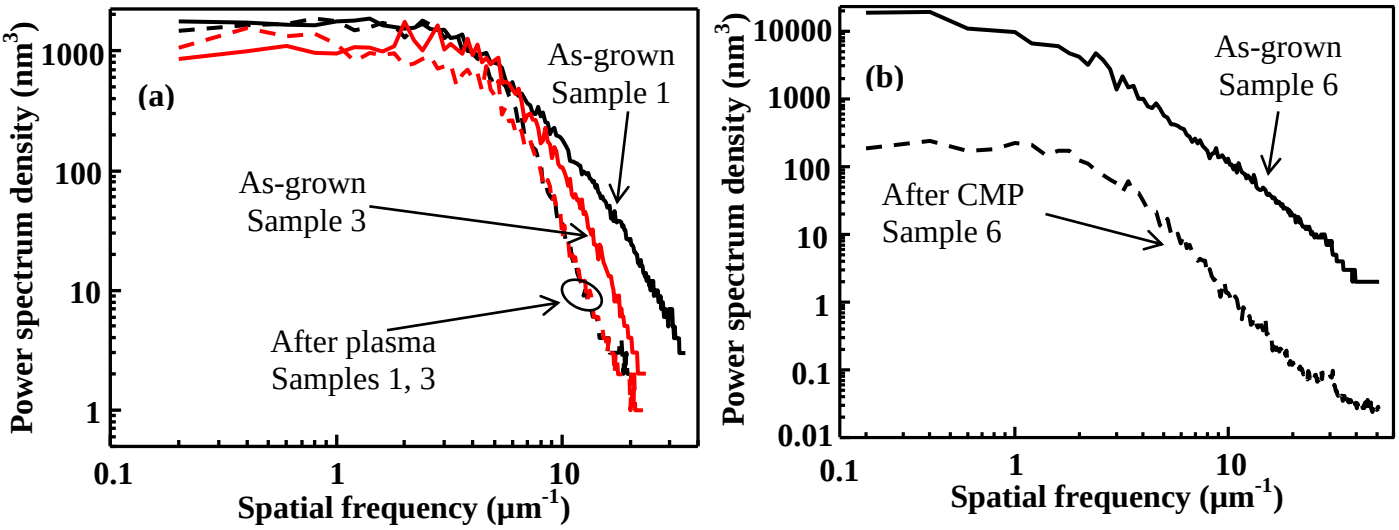

FIG. 6. Power spectral densities of 3C-SiC films on on-axis Si(111): (a) 250nm thick (sample 1 and 3), as-grown and after plasma smoothening and, (b) 1 μm thick, as-grown and after CMP. Whereas the CMP smoothens surface asperities over the full range of investigated frequencies, the plasma process smoothens selectively only the finest surface topography (spatial frequencies beyond 7 μm^{-1}).